Vol. 58: 55–66, 2013
doi: 10.3354/cr01189

CLIMATE RESEARCH
Clim Res

Published November 19

A dynamic control system model for global temperature change and sea level rise in response to CO_2 emissions

Jiabao Guan*, Biao Chang, Mustafa M. Aral

Multimedia Environmental Simulations Laboratory, School of Civil and Environmental Engineering, Georgia Institute of Technology, Atlanta, Georgia 30332, USA

ABSTRACT: Greenhouse gas emissions from natural and anthropogenic sources are frequently cited as the dominant cause of global warming. One adverse effect of global warming caused by these emissions is sea level rise, which poses a significant threat to the sustainable development of coastal regions around the world. In this study we use concepts from dynamic systems control theory to develop a systems model that may be used to predict global temperature change and sea level rise. The model uses the radiative forcing function as an external input to represent the impact of greenhouse gas emissions on the dynamic system. The dynamic system is calibrated using historical data on global temperature and sea level. An independent emission scenario, which results in a 2°C increase of temperature by 2100, is used to validate the model. The numerical results show that the model proposed is effective in predicting future global temperature change and future sea level rise. We then apply the proposed model to the 6 CO_2 emission scenarios generated by the Intergovernmental Panel on Climate Change (IPCC). The projections indicate that global temperature will increase between 1.6 and 5.0°C by 2100 and that sea level will rise between 60.3 and 98.4 cm relative to the 1990 level. These results are consistent with projections made by the IPCC and with results of other recent studies that used semi-empirical approaches.

KEY WORDS: Global warming · Sea level rise · Dynamic control system · Radiative forcing · Emission scenarios

1. INTRODUCTION

Sea level rise (SLR) caused by global warming poses a significant threat to the sustainable development of coastal regions around the world. In the past century, sea level has risen between 15 and 20 cm, (Douglas 1997, Church & White 2006), and in the 21st century it is predicted to rise faster due to an anticipated increase of natural and anthropogenic greenhouse emissions (Meehl et al. 2007). According to the Fourth Assessment Report by the Intergovernmental Panel on Climate Change (IPCC), the global mean surface temperature will likely rise by 1.1 to 6.4°C during the 21st century. It is anticipated that this temperature rise will cause the sea level to rise by 0.18 to 0.59 m by 2100 (IPCC 2001, 2007). These projections are viewed as an underestimation by some researchers (Rahmstorf 2007, 2010, Pfeffer et al. 2008, Vermeer & Rahmstorf 2009, Grinsted et al. 2010, Jevrejeva et al. 2010).

The physical mechanisms that influence global warming and SLR are complicated. Current physical-process models focus on the thermal expansion of sea water, continental ice sheet melting and the mass contribution of freshwater from the continents (Meehl et al. 2007). However, current scientific understanding of the dynamic behavior of ice sheets may be too

*Email: jg79@ce.gatech.edu

limited to permit accurate quantitative modeling (von Storch et al. 2008, Grinsted et al. 2010). Furthermore, the processes of thermal expansion and mass contribution are highly nonlinear, and the relationships between these processes are not well understood. These are some of the reasons why models based on physical processes may not be able to predict global temperature and sea level rise with sufficient accuracy (Vermeer & Rahmstorf 2009). It can be argued that the inherent relationship between global mean surface temperature and SLR is imbedded in the historical data, and models can be developed to exploit this information. Using this idea, scientists have developed a variety of empirical or semi-empirical models to relate climate change data to SLR and model SLR in the 21st century. The rationale behind the empirical modeling is that all major contributors to SLR are associated with temperature change (von Storch et al. 2008, Grinsted et al. 2010). By quantifying the correlation between SLR and temperature change, all known and unknown mechanisms of SLR can be modeled (von Storch et al. 2008).

Based on this approach, Etkins & Epstein (1982) formulated a linear relationship between the rate of SLR, temperature change and polar ice sheet mass change. They used this relationship to derive the polar ice sheet mass change from 1890 to 1980 and discussed the negative contribution of ice sheet melting to global warming. Gornitz et al. (1982) identified a linear correlation between sea level and global surface air temperature based on observational data from 1880 to 1980 and calculated the time lag between temperature change and SLR to be 18 yr, which is of the same order of magnitude as the thermal relaxation time for the upper layers of the ocean. Based on observed data sets for the period 1880 to 2001, Rahmstorf (2007) proposed a linear correlation between global average near-surface temperature and the rate of SLR, which he estimated to be 3.4 mm yr^{-1} $°C^{-1}$. This outcome was discussed in the literature with reference to the impact of the clustering and trending of the data on the model (Holgate et al. 2007, Schmith et al. 2007). In a subsequent study, Vermeer & Rahmstorf (2009) added a rapid-response term to Rahmstorf's (2007) original model. Inclusion of this term assumes that the rate of SLR is linearly proportional not only to the mean global temperature, but also to the rate of temperature rise. This addition makes the model better able to capture the short-term variability of sea level. Vermeer & Rahmstorf (2009) used this model to calibrate observation data that had been corrected for human reservoir construction and discovered a time lag of 13 yr between SLR and temperature change. Grinsted et al. (2010) constructed a semi-empirical model of SLR by assuming a linear relationship between a given temperature and the corresponding equilibrium sea level, which they argue would be a valid approximation for the late Holocene-Anthropocene climate. Their model quantified the rate of SLR as the difference between the equilibrium sea level and current sea level divided by a characteristic response time (Grinsted et al. 2010). This model was modified in a subsequent study by Jevrejeva et al. (2009, 2010) by replacing the temperature term with its corresponding mean global radiative forcing. When these models are used, the projections of SLR in the 21st century generally fall between 0.5 and 2.0 m.

In the empirical models reviewed above, the temperature series derived from IPCC greenhouse gas emission scenarios were used as known inputs to predict the SLR. As an alternative to empirical methods, Aral et al. (2012) proposed a model that relied on dynamic system analysis. In their study they regarded the earth as a system and expressed its behavior in terms of 2 state variables, temperature and sea level. In their approach the evolution of both states depended only on the current state of the system, as opposed to the system's state at previous times. Unlike in previous methods, the earth system in their model was described in terms of 2 coupled state equations, which allowed for the simultaneous prediction of both temperature and SLR for a given initial state. Relative to 1990 measurements, they predicted an increase in temperature of about 1.3°C by 2100, with a 90% confidence interval of [1.1, 1.5]°C. They also predicted a SLR of about 42.4 cm over the same time period, with a 90% confidence interval of [40.0, 44.8] cm. These predictions were based on the assumption that the future relationship between temperature and SLR would be consistent with the relationship observable from historical records (Aral et al. 2012). As they discussed, their model did not separate the influence of radiative forcing from that of temperature, which may produce errors in prediction if the future natural and anthropogenic gas emissions are different from the pattern identified from historical observations. Most recently an independent vector-autoregressive (VAR) model was developed that uses a stochastic cointegration method to describe the relationship between surface temperature and sea level (Schmith et al. 2012). This model has the same structure as the discrete dynamic systems model used by Aral et al. (2012), and the results of their study confirm a hypothesis underlying the dynamic systems model used in Aral et al. (2012), as stated in Schmith et al. (2012), that surface air temperatures will adjust to the average temperatures of the upper ocean due to the larger heat capacity of oceans relative to the atmosphere. As a result of this difference in heat capacities, SLR will directly affect temperature. It is known that temperature change will affect SLR due to ice sheet melting and other hydrologic changes, the information on which is imbedded in the historical data on SLR and temperature change.

Considering that natural and anthropogenic radiative forcing may change in the future as a function of economic and industrial development and population growth, in this study we develop a new dynamic control system model for global temperature change and SLR based on system control theory. The model uses the radiative forcing functions generated from greenhouse gas emissions as external system inputs to incorporate the impact of radiative forcing on global warming and SLR. We use the historical temperature and SLR data from 1880 to 2001 and the radiative forcing calculated from CO_2 concentration data provided by the IPCC to calibrate the model, and then use the independent '2°C' emission scenario of Hansen et al. (2000) as an example to demonstrate the model's effectiveness. Finally we apply the calibrated model to 6 special emission scenarios generated by the IPCC (2001, 2007) to predict the temperature and SLR in the 21st century.

2. DYNAMIC CONTROL SYSTEM MODEL

2.1. Model description

The hypothesis in this model is that the rates of change of global temperature and SLR depend both on their states and on the radiative forcing from natural and anthropogenic emissions, which is introduced as an external forcing on the system. Defining the global temperature and SLR as the 2 state variables and radiative forcing through external input parameters, or control variables in systems analysis terminology, we develop a dynamic control system model for global temperature and SLR. In the dynamic control system we define:

$$\left.\begin{aligned} &\boldsymbol{X}(t) = (T(t),\, H(t))^{\tau} \\ &\frac{\mathrm{d}\boldsymbol{X}(t)}{\mathrm{d}t} = \left(\frac{\mathrm{d}T(t)}{\mathrm{d}t}, \frac{\mathrm{d}H(t)}{\mathrm{d}t}\right)^{\tau} \\ &\boldsymbol{U}(t) = (u_1(t), u_2(t), \cdots, u_m(t))^{\tau} \end{aligned}\right\} \quad (1)$$

where $\boldsymbol{X}(t)$ is the state vector, $\frac{\mathrm{d}\boldsymbol{X}(t)}{\mathrm{d}t}$ is the rate vector for temperature change and SLR, $\boldsymbol{U}(t)$ is the external forcing vector, t is time, $T(t)$ is the global mean surface temperature at time t, $H(t)$ is global sea level at time t, m is the number of external forcing functions, u_j is a radiative forcing function introduced from greenhouse gas emission j, where $j = 1,\ldots,m$, and τ is the transpose operator. Radiative forcing (RF) is used to assess and compare the anthropogenic and natural drivers of climate change. It is a measure that can be used for both quantifying and ranking many different influences on climate change, including greenhouse gases (IPCC 2001, 2007). The RF introduced from CO_2 concentrations can be estimated from a simplified expression given by (IPCC 2001):

$$\mathrm{RF}_{CO_2} = 5.35 \ln(C/C_0) \quad (2)$$

Accordingly, u_{CO_2} in the dynamic control system model can be defined as:

$$u_{CO_2} = (\mathrm{RF}_{CO_2})^{\beta} \quad (3)$$

where RF_{CO_2} represents the radiative forcing introduced from CO_2 (W m^{-2}), C is the CO_2 concentration (ppmv), C_0 is the baseline value of CO_2 concentration and is given as 278 ppmv, and β is an exponent for RF_{CO_2}. The coefficient β reflects the influence of RF_{CO_2} on the system and needs to be identified. The system described above can be approximated using a dynamic control system equation given by:

$$\frac{\mathrm{d}\boldsymbol{X}(t)}{\mathrm{d}t} = \mathbf{A}\boldsymbol{X}(t) + \mathbf{B}\boldsymbol{U}(t) + \mathbf{C} + \mathbf{w}(t) \quad (4)$$

where $\mathbf{A}$ is a 2×2 system matrix associated with the state variables, $\mathbf{B}$ is a $2 \times m$ control matrix related to external forcing functions, $\mathbf{C}$ is a 2×1 constant vector and $\mathbf{w}(t)$ is the error vector. In Eq. (4), the term $\mathbf{A}\boldsymbol{X}(t)$ represents the interactions of the intrinsic states of the system on the rates of temperature change and SLR, the term $\mathbf{B}\boldsymbol{U}(t)$ reflects the total impact of external radiative forcing functions on the evolution of the system, and the term $\mathbf{C}$ characterizes the relationship between state variables and radiative forcing for the equilibrium states.

The matrices $\mathbf{A}$ and $\mathbf{B}$ and the vector $\mathbf{C}$ are given by:

$$\mathbf{A} = \begin{bmatrix} a_{11} & a_{12} \\ a_{21} & a_{22} \end{bmatrix}, \mathbf{B} = \begin{bmatrix} b_{11} & b_{12} & \cdots & b_{1m} \\ b_{21} & b_{22} & \cdots & b_{2m} \end{bmatrix}, \mathbf{C} = \begin{Bmatrix} c_1 \\ c_2 \end{Bmatrix} \quad (5)$$

where a_{ij} denotes the effect of state variable j on state variable i, and b_{ij} reflects the impact of the external forcing function j on state variable i. The matrix $\mathbf{A}$ and the vector $\mathbf{C}$ given above are similar to those defined in Aral et al. (2012), except that in the current model the coefficients of $\mathbf{A}$ and $\mathbf{C}$ exclude the impact of the external forcing function, which is now included in the coefficients of the matrix $\mathbf{B}$.

The system described above can be discretized into a discrete dynamic control system:

$$\boldsymbol{X}(k+1) = \boldsymbol{\Phi}\boldsymbol{X}(k) + \boldsymbol{\Gamma}\boldsymbol{U}(k) + \boldsymbol{\Omega} + \mathbf{w_1}(k) \tag{6}$$

where k is time step, $\mathbf{X}(k)$ indicates the values of temperature and SLR in time step k, $\boldsymbol{U}(k)$ indicates the values of external forcing functions in time step k, $\mathbf{w_1}(k)$ is the error vector in the discrete control system, $\boldsymbol{\Phi}$ is a (2×2) system matrix, $\boldsymbol{\Gamma}$ is a $(2 \times m)$ control matrix for external forcing functions, and $\boldsymbol{\Omega}$ is a (2×1) constant vector. Both systems satisfy the relationships:

$$\boldsymbol{\Phi} = \mathbf{I} + \mathbf{A}\Delta t, \quad \boldsymbol{\Gamma} = \mathbf{B}\Delta t, \quad \boldsymbol{\Omega} = \mathbf{C}\Delta t \tag{7}$$

where Δt is the time step length and $\mathbf{I}$ is the identity matrix. This system can now be calibrated using the historical data on temperature, SLR and emissions.

2.2. System calibration

The system can be calibrated using the least squares method based on the historical data for temperature, SLR and forcing functions. Assuming that there are $(N+1)$ sets of time series data $[T(k), H(k), u_1(k),\ldots,u_\mathrm{m}(k)], k = 0,1,\ldots,N)$ available, these data sets can be used to form the matrices:

$$\boldsymbol{\Pi} = \begin{bmatrix} T(0) & H(0) & u_1(0) & \cdots & u_m(0) & 1 \\ T(1) & H(1) & u_1(1) & \cdots & u_m(1) & 1 \\ \vdots & \vdots & \vdots & \vdots & \vdots & \vdots \\ T(N-1) & H(N-1) & u_1(N-1) & \cdots & u_m(N-1) & 1 \end{bmatrix},$$

$$\mathbf{Y} = \begin{bmatrix} T(1) & H(1) \\ T(2) & H(2) \\ \vdots & \vdots \\ T(N) & H(N) \end{bmatrix} \tag{8}$$

and unknown parameters in the system are expressed as a parameter matrix $\mathbf{P}$, defined as:

$$\mathbf{P} = \begin{Bmatrix} \varphi_{11} & \varphi_{12} & \gamma_{11} & \cdots & \gamma_{1m} & \omega_1 \\ \varphi_{21} & \varphi_{22} & \gamma_{21} & \cdots & \gamma_{2m} & \omega_2 \end{Bmatrix} \tag{9}$$

where ϕ_{ij} is a coefficient in row i and column j of matrix $\boldsymbol{\Phi}$, γ_{ij} is a coefficient in row i and column j of matrix $\boldsymbol{\Gamma}$, and ω_i is a coefficient in row i of vector $\boldsymbol{\Omega}$. Applying the least squares method, the estimator of $\mathbf{P}$, denoted as $\hat{\mathbf{P}}$, is given by:

$$\hat{\mathbf{P}} = [(\boldsymbol{\Pi}^\tau\boldsymbol{\Pi})^{-1}\boldsymbol{\Pi}\mathbf{Y}]^\tau \tag{10}$$

In matrix $\hat{\mathbf{P}}$, the first 2 columns consist of the estimator of $\boldsymbol{\Phi}$, denoted as $\hat{\boldsymbol{\Phi}}$, the following m columns consist of the estimator of $\boldsymbol{\Gamma}$, denoted as $\hat{\boldsymbol{\Gamma}}$ and the last column consists of the estimator of the vector $\boldsymbol{\Omega}$, denoted as $\hat{\boldsymbol{\Omega}}$, where the symbol ˆ over a variable indicates the estimator of the variable. Therefore, the resulting discrete dynamic control system is given by:

$$\hat{\boldsymbol{X}}(k+1) = \hat{\boldsymbol{\Omega}}\boldsymbol{X}(k) + \hat{\boldsymbol{\Gamma}}\boldsymbol{U}(k) + \hat{\boldsymbol{\Omega}} \tag{11}$$

Based on the discrete solution the continuous dynamic control system can be easily obtained using the relations given in Eq. (7).

As stated above, the system contains various uncertainties such as modeling uncertainty, measurement errors and the effect of other random factors. Confidence interval analysis may be used to evaluate the effect of such uncertainties on the outcome (Wadsworth 1998). For a given confidence level α, the (1 – α)% confidence intervals of projected temperature and SLR can be estimated by:

$$\left.\begin{aligned} T_c(k) &= \hat{T}(k) \pm t_{\alpha/2,N-3}\sigma_T\sqrt{1+\mathbf{X}_p^\tau(k)(\boldsymbol{\Pi}^\tau\boldsymbol{\Pi})^{-1}\mathbf{X}_p(k)} \\ H_c(k) &= \hat{H}(k) \pm t_{\alpha/2,N-3}\sigma_H\sqrt{1+\mathbf{X}_p^\tau(k)(\boldsymbol{\Pi}^\tau\boldsymbol{\Pi})^{-1}\mathbf{X}_p(k)} \end{aligned}\right\} \tag{12}$$

where $T_c(k)$ and $H_c(k)$ represent the interval of temperature and SLR at time step k, σ_T and σ_H are respectively the standard deviations of temperature and SLR, estimated from historical data, and $\boldsymbol{X}_p(k)$ is defined as:

$$\boldsymbol{X}_p(k) = [\hat{T}(k-1), \hat{H}(k-1),\ u_1(k-1),\ldots,u_\mathrm{m}(k-1), 1]^\tau \tag{13}$$

2.3. Evaluation of model

The root mean square error (RMSE) and the coefficient of determination (R^2) are 2 indicators that are frequently used to evaluate the performance of a model. The RMSE is a measure of the differences between values predicted by the model and the actual observations (Anderson & Woessner 1992). It is defined as:

$$\left.\begin{aligned} \mathrm{RMSE}_T &= \sqrt{\frac{1}{N}\sum_{k=1}^{N}\left(T(k)-\hat{T}(k)\right)^2} \\ \mathrm{RMSE}_H &= \sqrt{\frac{1}{N}\sum_{k=1}^{N}\left(H(k)-\hat{H}(k)\right)^2} \end{aligned}\right\} \tag{14}$$

where RMSE_T and RMSE_H are the root mean square errors for temperature and SLR, and $T(k)$ and $H(k)$ are the historical measurements of temperature and SLR at time step k. The smaller the RMSE, the better the goodness of fit.

The coefficient of determination R^2 is a measure of how well future outcomes are likely to be predicted by a model (Draper & Smith 1998). The R^2 is defined as:

$$\left.\begin{aligned} R_T^2 &= \sum_{k=1}^{N}\left(\hat{T}(k)-\bar{T}\right)^2 \bigg/ \sum_{k=1}^{N}\left(T(k)-\bar{T}\right)^2 \\ R_H^2 &= \sum_{k=1}^{N}\left(\hat{H}(k)-\bar{H}\right)^2 \bigg/ \sum_{k=1}^{N}\left(H(k)-\bar{H}\right)^2 \end{aligned}\right\} \quad (15)$$

where R_T^2 and R_H^2 are the coefficients of determination for temperature and SLR, and $\bar{T}$ and $\bar{H}$ are the average values of the observations of temperature and SLR, defined as $\bar{T} = \frac{1}{N}\sum_{k=1}^{N} T(k)$ and $\bar{H} = \frac{1}{N}\sum_{k=1}^{N} H(k)$. The closer that the value of R^2 is to one, the better the linear regression fits the data in comparison to the simple average. Both RMSE and R^2 were used to evaluate the performance of the system expressed in Eq. (4).

2.4. Applications

In this study, we apply the historical dataset on temperature and SLR, and the CO_2 emission data obtained from IPCC scenarios to calibrate the system model. The historical dataset, used in Aral et al. (2012), includes yearly records of global mean temperature (°C) and sea levels (cm) from 1880 to 2001. The emission data from the IPCC scenarios include yearly historical records of CO_2 concentrations (ppmv) from 1880 to 2001 and projections of CO_2 concentrations from 2002 to 2100 for different emissions scenarios. Among various gases emitted, CO_2 is a dominant contributor to future global warming (Hansen et al. 2000). In this study, for simplicity and without loss of generality, we will focus on the impact of the radiative forcing introduced from CO_2 emission only on the dynamic system behavior.

The system calibration is based on a 2 yr moving average of the historical data from 1880 to 2001. The radiative forcing introduced from CO_2 concentrations is calculated by Eq. (2) and the corresponding external input acting on the system is defined by Eq. (3). The golden cut approach coupled with the least squares method is used to identify the exponent β and the system matrix coefficients. In the golden cut approach, minimizing total RMSE for temperature and SLR is chosen as the objective function. During the golden cut iteration, u_{CO_2} is calculated using Eq. (3) for a given β, and then the system matrices can be calibrated using the least squares method as described earlier. Through an iterative analysis, the optimal value of β is obtained as 1.31:

$$u_{CO_2} = (RF_{CO_2})^{1.31} \quad (16)$$

The calibrated system coefficients are listed in Table 1. From the discrete system, it can be seen that the temperature change is proportional to both the temperature state in the previous year and the current sea level state, with constants of 0.75572°C °C^{-1} and 0.00057°C cm^{-1}, respectively. The radiative forcing function introduced from CO_2 concentrations causes temperature to increase at a rate of 0.10584°C (W m^{-2})$^{-1}$. The SLR is proportional to both temperature and sea level states of the previous year with coefficients 0.41015 cm °C^{-1} and 0.99568 cm cm^{-1}, respectively, while the radiative forcing has no direct impact on SLR. Using Eq. (7), we can also obtain the corresponding continuous system, the coefficients of which are listed in Table 1. The coefficients of the continuous system indicate that the rates of temperature change and SLR are negatively related to their states and that the system is a negative feedback system. This observation reveals the fundamental mechanism of the dynamic control system's operation. That is, as temperature and sea level increase, their rates of change will decrease. However, the radiative forcing will accelerate temperature change, which in turn will affect SLR. This impact of radiative forcing also implies that reducing greenhouse gas emissions would be an effective way to reduce both global warming and SLR. This outcome also provides an explanation of why historical data on temperature and sea levels do not increase monotonically, even though CO_2 emissions have increased consistently over the years.

The other important outcome of the dynamic control system analysis is the estimation of the effect of

Table 1. Calibrated system coefficients based om least square method

System	System matrix	Control matrix	Constant vector
Discrete	$\begin{bmatrix} 0.75572\ (°C\ °C^{-1}) & 0.00057\ (°C\ cm^{-1}) \\ 0.41015\ (cm\ °C^{-1}) & 0.99568\ (cm\ cm^{-1}) \end{bmatrix}$	$\begin{bmatrix} 0.10584\ (°C\ W^{-1}\ m^{-2}) \\ 0 \end{bmatrix}$	$\begin{Bmatrix} -0.14041\ (°C) \\ 0.25863\ (cm) \end{Bmatrix}$
Continuous	$\begin{bmatrix} -0.24428\ (°C\ °C^{-1}\ yr^{-1}) & 0.00057\ (°C\ cm^{-1}\ yr^{-1}) \\ 0.41015\ (cm\ °C\ yr^{-1}) & -0.00432\ (cm\ cm^{-1}\ yr^{-1}) \end{bmatrix}$	$\begin{bmatrix} 0.10584\ (°C\ W^{-1}\ m^{-2}\ yr^{-1}) \\ 0 \end{bmatrix}$	$\begin{Bmatrix} -0.14041(°C\ yr^{-1}) \\ 0.25863(cm\ yr^{-1}) \end{Bmatrix}$

controlling radiative forcing on the system behavior. For example, based on the system equation calibrated, if we want to restrict the global temperature and SLR rise to zero-growth ($dX/dt = 0$), from Eqs. (2) to (4), the global CO_2 concentration in the atmosphere should be controlled with the relationship given by:

$$C(t) = 278\exp\{0.186916[2.30812T(t) - 0.00542H(t) + 1.32668)^{0.76336}]\} \quad (17)$$

where $C(t)$ represents the CO_2 concentration (ppmv) at year t. For example, if the desire is to keep the future temperature and SLR at 1990 levels, then $T(1990)$ and $H(1990)$ should be set to zero to establish 1990 as the baseline. Substituting both values into Eq. (17) will give the required CO_2 concentration in the atmosphere to maintain 1990 levels of temperature and SLR. According to Eq. (17) the CO_2 concentrations (ppmv) should be kept at about 350.6 ppmv. This value is very close to the actual CO_2 concentration in 1990, which is 354.3 ppmv in the historical data. Given this exercise, the temperature and sea levels of any other year can be used in Eq. (17) to determine the CO_2 control necessary on the system.

The calibrated system was used to reconstruct the dynamic temperature and sea levels from 1880 to 2001 relative to 1990 levels, and the results are shown in Fig. 1. It can be noticed that the historical data for both temperature and sea level are fitted accurately using the model developed. The RMSEs are 0.09 and 0.92, and the R^2 are 0.80 and 0.97 for temperature and SLR, respectively. In comparison with the results reported in Aral et al. (2012), the performance of the dynamic system significantly improves when the external radiative forcing function based on CO_2 concentrations is introduced. The 90% confidence intervals were estimated using Eq. (12), and the results are shown as dashed lines in Fig. 1. It can be seen that this band envelopes more than 90% of the historical data points.

In order to further evaluate the performance of the model, a 10-fold cross-validation technique is applied

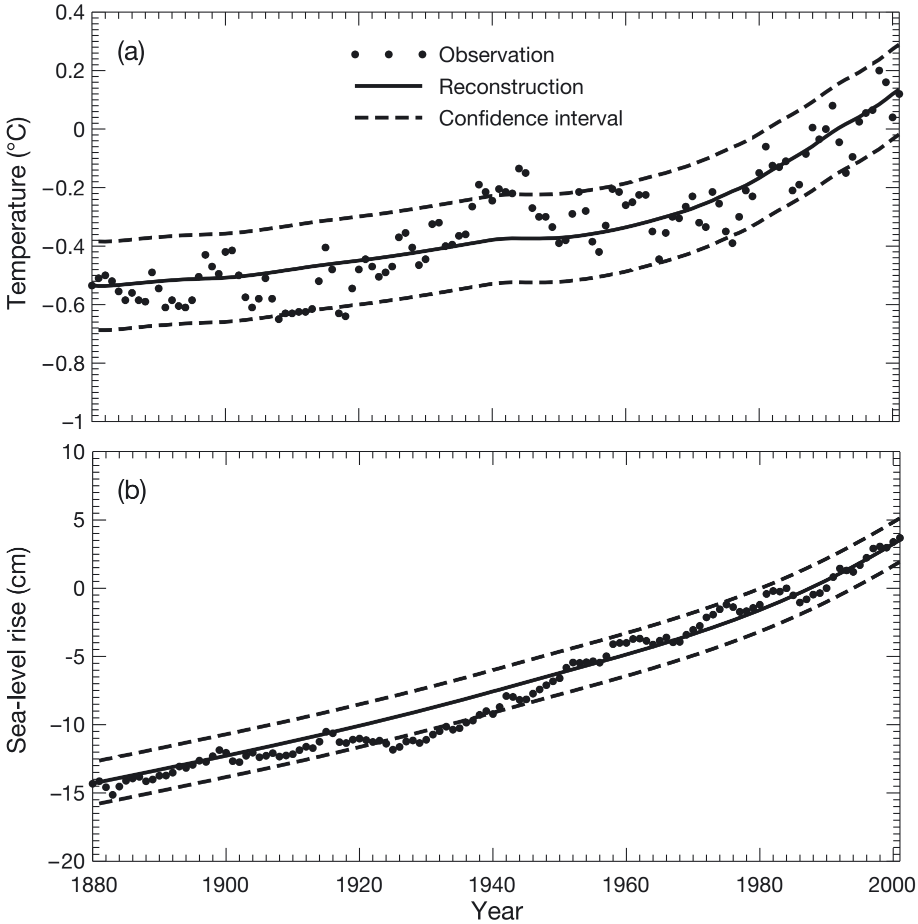

Fig. 1. Reconstructed temperature and sea level rise (SLR) from 1880 to 2001 using the dynamic control system model, compared with observational data

to the measured dataset of temperature and SLR from 1880 to 2001 (McLachlan et al. 2004). In this cross-validation technique, the dataset is randomly divided into 10 equal subgroups. Of the 10 subgroups, a single subgroup is retained as the validation data for testing the model while the remaining 9 subgroups are used to identify the model. This process is repeated 10 times, and the resultant parameters of the model are averaged to produce a single estimation. When we used this process to reconstruct the dynamic temperature and sea levels from 1880 to 2001 relative to 1990 levels, the resulting RMSEs were 0.12 and 1.07, and the R^2 are 0.65 and 0.96 for temperature and SLR, respectively. These values are very close to the results obtained from the model calibrated using the complete dataset.

An independent scenario, identified as the '2 °C' scenario, is used to further verify the model calibrated above. This scenario is designed to limit global warming in 2100 to 2°C above the temperature in 2000 (Hansen et al. 2000, 2007, Hansen & Sato 2004). Using the temperature and sea level in 1990 as the initial condition and the yearly CO_2 concentration data provided in this scenario to calculate the radiative forcing by Eq. (2), the calibrated system was used to predict the temperature and SLR rise in the 21st century. The results are shown in Fig. 2. In 2100, temperature increases 2.0044°C with a 90% confidence interval of [1.77, 2.24]°C while SLR reaches 63.62 cm with a 90% confidence interval of [61.14, 66.09] cm. When compared with the temperature in 2100 in the 2°C scenario, the predicted temperature has an absolute difference of 0.0044°C and a relative difference of 0.22%. When the predicted temperature is applied to the semi-empirical approach proposed by Rahmstorf (2007), the prediction is that the sea level will rise 68.14 cm by 2100. The difference between these results is 4.52 cm, with the dynamic system model results being lower. These comparisons for the 2°C scenario indicate that the model proposed is effective in projecting temperature and SLR in the 21st century.

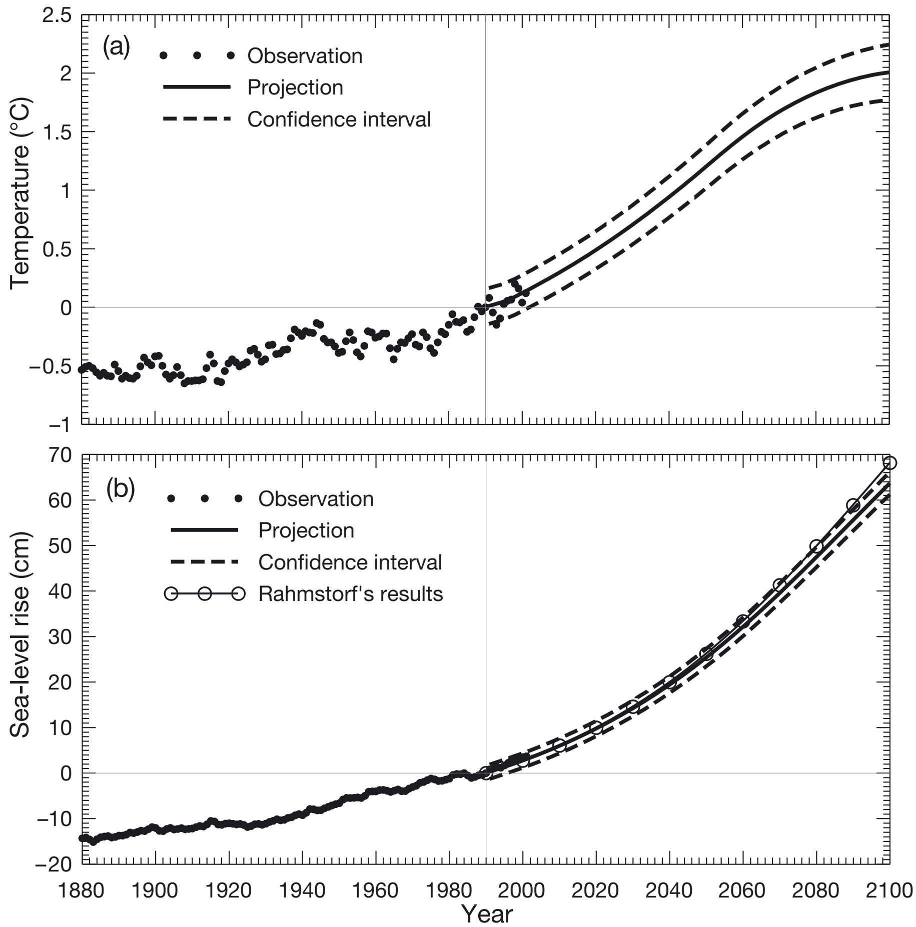

Fig. 2. Projected temperature and sea level rise (SLR) from 1990 to 2100 using the dynamic control system model for the '2°C' scenario (Hanson et al. 2000, 2007) and corresponding observational data covering the period 1880 to 2001

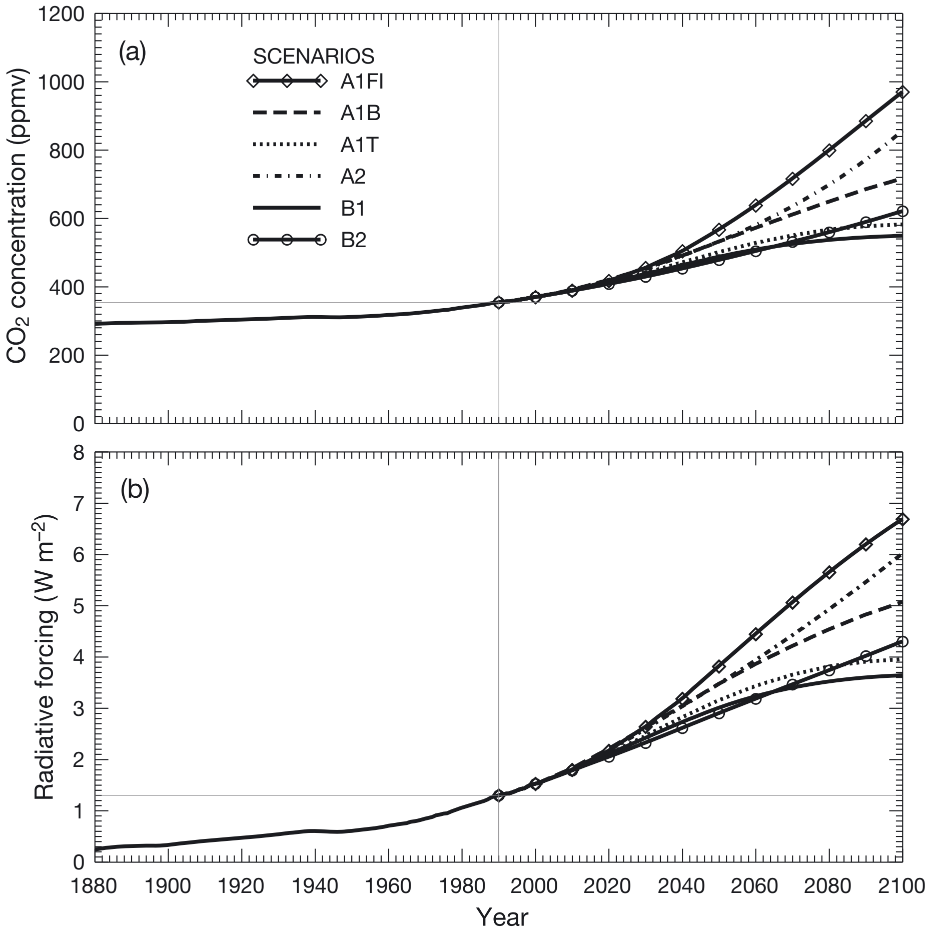

Fig. 3. CO_2 concentrations and radiative forcing for the 6 IPCC CO_2 emission scenarios (IPCC 2001, 2007)

In order to assess the impact of greenhouse gas emissions on global warming, the IPCC developed 6 emission scenarios (Special Report on Emission Scenarios—SRES) based on different patterns of economic development, industrial development, and population growth in the future and modeled physical processes (IPCC 2001, 2007). These emission scenarios are labeled A1FI, A1B, A1T, A2, B1 and B2 (IPCC 2001). In group A1 (A1FI, A1B and A1T), it is assumed that the global economy expands rapidly and population growth is low, producing a wide range in CO_2 emissions for different strategies of energy supply. The scenario A1FI represents a heavy reliance on fossil fuels, while the scenario A1B has a more balanced energy portfolio with a mixture of both clean and fossil-fuel energies. The scenario A1T represents the continual expansion of non-carbon energy production to 85% by 2100. In scenario A2, it is assumed that economic growth is both slower and more geographically varied than it is for scenario A1. Additionally, population growth is high, resulting in medium to high CO_2 emissions. In the scenario B1, widespread economic growth increases wealth and reduces the income disparity between rich and poor nations, and a switch to clean and efficient forms of energy production result in the lowest CO_2 emissions of the 6 scenarios. In scenario B2, it is assumed that economic development is moderate, that population growth continues to increase but slows in the second half of the 21st century, and that clean technologies are slowly integrated into society, resulting in a moderate reduction of CO_2 emissions. Among these scenarios, A1FI and A2 represent the highest emission of greenhouse gases into the atmosphere, A1T and B1 represent the least emissions, and A1B and B2 represent moderate emissions. According to the IPCC, each scenario has the same probability of occurrence, but current emissions will outpace the worst emission scenario, A1FI, if the burning of fossil fuels continues at its current level (IPCC 2001). The projection of CO_2 concentrations in these 6 scenarios and the corresponding radiative forcing are shown in Fig. 3.

Choosing the temperature and sea level in 1990 as the initial condition and the yearly radiative forcing

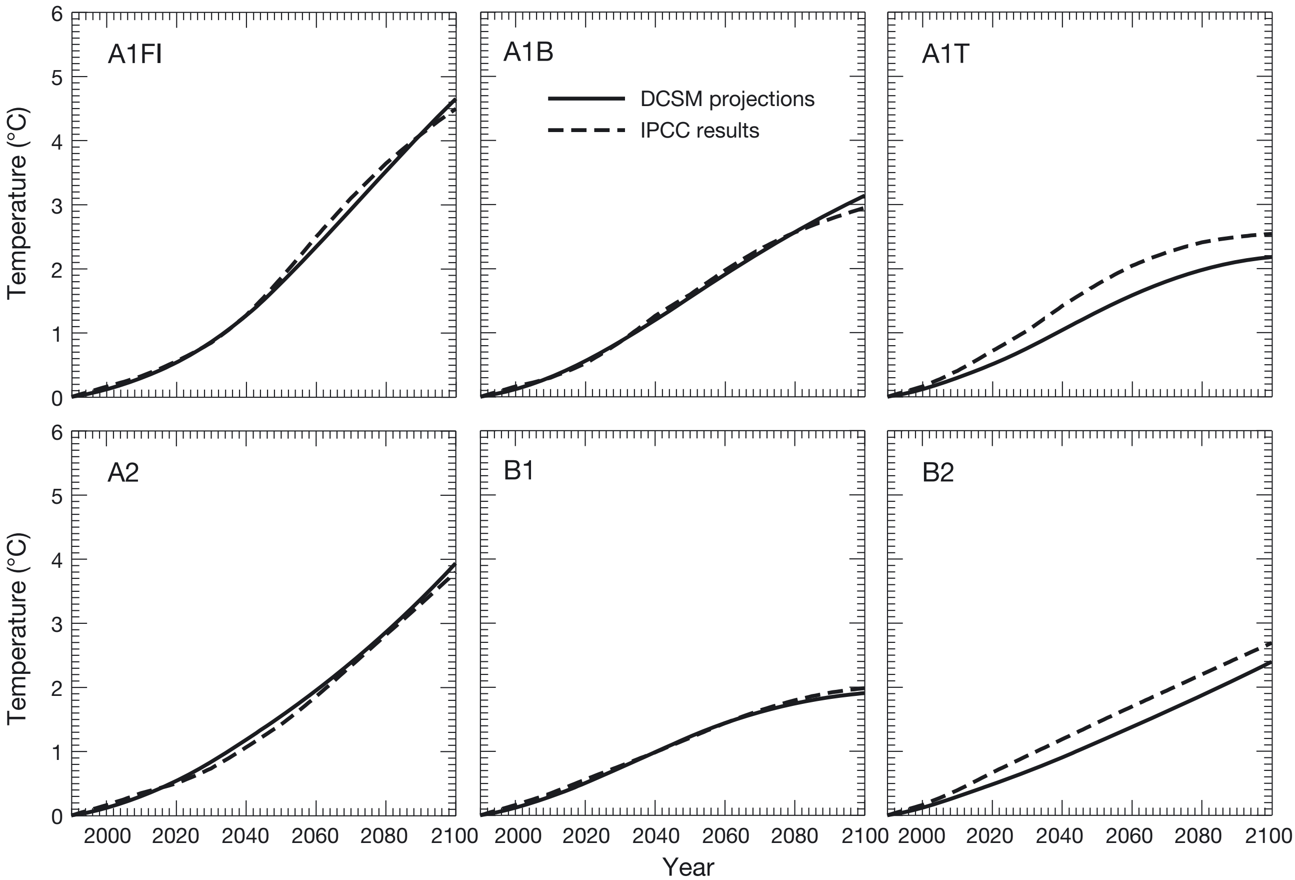

Fig. 4. Predicted temperature from 1990 to 2100 using the dynamic control system model for the IPCC CO_2 emission scenarios, compared with the temperature projections reported by the IPCC

calculated from the 6 scenarios as known inputs, the system model was applied to predict the global temperature and SLR in the 21st century. The results are shown as solid lines in Figs. 4 & 5. For comparison purposes, the temperature projections of the 6 scenarios reported by the IPCC are also shown as dashed lines in Fig. 4, whereas the projections of SLR made by the semi-empirical approach (Rahmstorf 2007) are illustrated by dashed lines in Fig. 5. From these figures, we may observe that the temperature projected by the dynamic system model is consistent with the projections given by IPCC and that the projected SLR is comparable to the results of the semi-empirical approach (Rahmstorf 2007).

The temperature and SLR by 2100 predicted by the dynamic system model for all 6 IPCC scenarios are summarized in Tables 2 & 3. For the temperature by 2100, the estimates from the dynamic system model yield relative differences of 2.2, 3.3, 12.0, 2.6, 5.0 and 11.1% for the A1FI, A1B, A1T, A2, B1 and B2 scenarios respectively when compared with IPCC projections. All of the results are within the IPCC confidence intervals for each scenario. For the SLR by 2100, the best estimates from the dynamic system model are higher than the IPCC projections, and they are close to but consistently lower than the projections obtained by the semi-empirical approach (Rahmstorf 2007). For a given $\alpha = 10\%$, the 90% confidence intervals of temperature for 6 IPCC scenarios can be calculated using Eq. (12). The confidence intervals of temperature by 2100 obtained from the dynamic system model contain the IPCC best estimates but are narrower than those projected by the IPCC. Overall, by the year 2100 the dynamic system model predicts a temperature increase between 1.6 and 5.0°C and a SLR between 60.3 and 98.4 cm.

3. DISCUSSION AND CONCLUSIONS

In this study, a dynamic control system model is developed to predict both global temperature change and SLR in the 21st century. In the model, global temperature and SLR are the state variables of the sys-

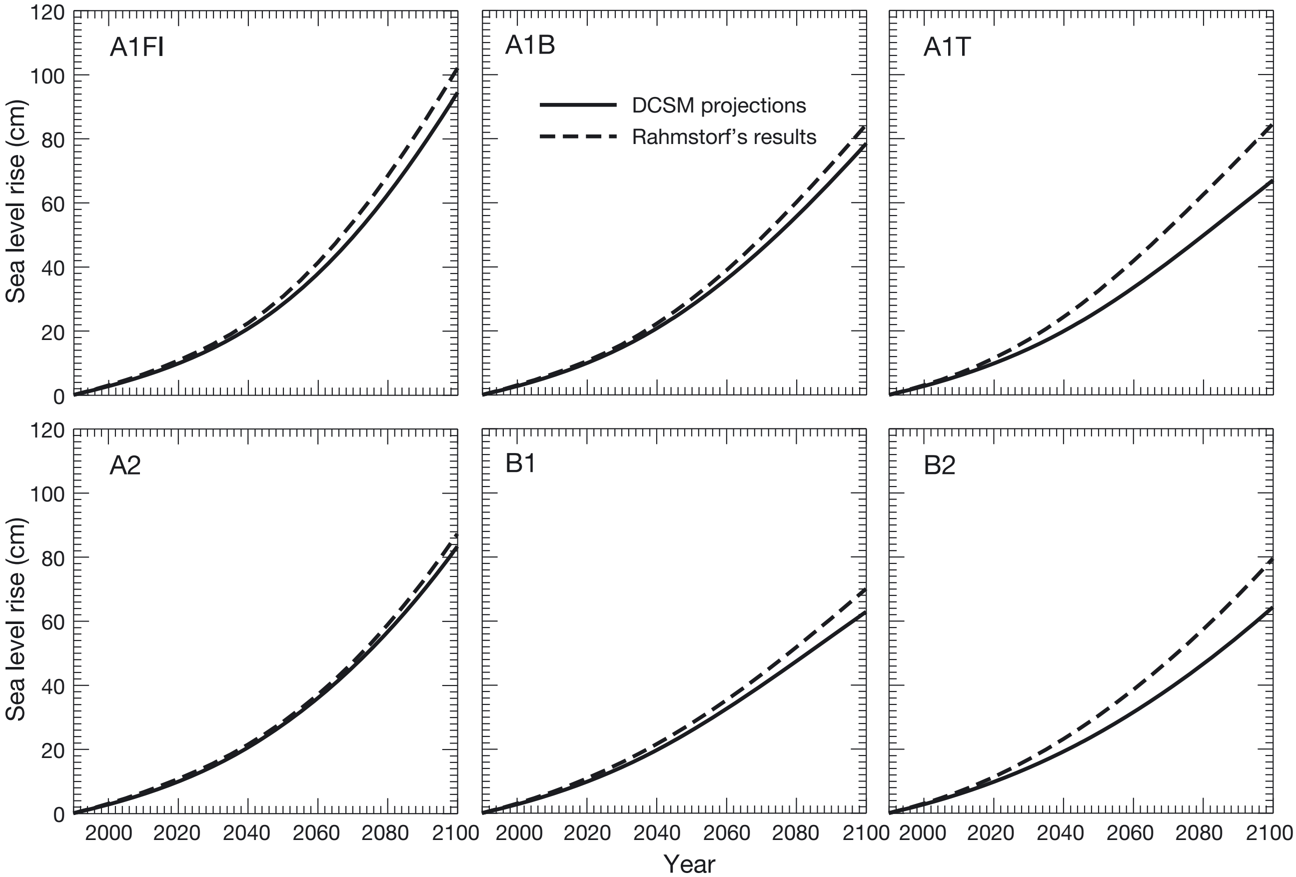

Fig. 5. Predicted SLR from 1990 to 2100 using the dynamic control system model for the IPCC CO_2 emission scenarios, compared with estimations using the semi-empirical approach of Rahmstorf (2007)

tem while radiative forcing from greenhouse gas emissions is considered through control variables acting on the system. Historical data were used to calibrate the system matrix coefficients, and the results show that temperature change and SLR are directly related and that temperature change is proportional to the radiative forcing function introduced from CO_2 concentrations with a rate of 0.10584°C $(W\ m^{-2})^{-1}\ yr^{-1}$. When the calibrated model is applied to 6 IPCC CO_2 emission scenarios the temperature is projected to increase between 1.6 and 5.0°C by 2100. These results are consistent with the projections reported in the IPCC studies. Although the dynamic interaction between temperature and SLR is a complex nonlinear system, the dynamic control system model discussed in this study can be regarded as a

Table 2. Temperature (°C) at the end of the 21st century predicted by the dynamic control system model for 6 IPCC CO_2 emission scenarios (IPCC 2001, 2007), compared with the projections reported by the IPCC

Scenario	Temperature change in 2100 relative to 1990			
	Best estimate	90% CI	IPCC projections Best estimate	IPCC projections Interval
A1FI	4.6	[4.2, 5.0]	4.5	[2.4, 6.4]
A1B	3.1	[2.8, 3.4]	3.0	[1.7, 4.4]
A1T	2.2	[1.9, 2.5]	2.5	[1.4, 3.8]
A2	3.9	[3.5, 4.3]	3.8	[2.0, 5.4]
B1	1.9	[1.6, 2.1]	2.0	[1.1, 2.9]
B2	2.4	[2.1, 2.7]	2.7	[1.4, 3.8]

Table 3. Sea level rise (SLR, cm) at the end of the 21st century predicted by the dynamic control system model for the IPCC CO_2 emission scenarios (IPCC 2001, 2007), compared with predictions of SLR estimated by the semi-empirical approach of Rahmstorf's projections (Rahmstorf 2007) and those reported by the IPCC

Scenario	SLR in 2100 relative to 1990			
	Best estimate	90% CI	Rahmstorf's projections	IPCC projections
A1FI	94.4	[90.4, 98.4]	102.1	[26, 59]
A1B	78.5	[75.4, 81.4]	84.4	[21, 48]
A1T	67.0	[64.8, 69.6]	84.7	[20, 45]
A2	83.3	[79.8, 86.8]	87.2	[23, 51]
B1	62.8	[60.3, 65.3]	70.0	[18, 38]
B2	64.3	[61.7, 66.8]	79.5	[20, 43]

linearized model of this system in which the radiative forces are treated as external forcing functions. The proposed model belongs to the category of semi-empirical models, and it can be used to predict the global temperature and SLR simultaneously. Although the estimated temperatures obtained from the proposed model exhibit some differences when compared to the projections obtained from the physical model developed by IPCC, these differences are acceptable and can be further reduced through the use of a higher order dynamic control system model. The SLR projections by 2100 from the dynamic system model range between 0.63 and 0.94 m with a 90% confidence interval of [0.60, 0.98] m. The IPCC analysis suggested SLR between 0.18 and 0.59 m by 2100 (IPCC 2007) while subsequent studies show SLR by 2100 that ranges between 0.5 and 1.4 m (Rahmstorf 2007), 0.75 and 1.90 m (Vermeer & Rahmstorf 2010), 0.8 and 2.0 m (Pfeffer et al. 2008), 0.8 and 1.3 m (Grinsted et al. 2010) and 0.59 and 1.8 m (Jevrejeva et al. 2010). In comparison with these results, the predictions obtained from the dynamic system model are higher than those given by IPCC but lower than the results projected from the semi-empirical model studies. Based on the predicted results and analyses, we may draw the following conclusions:

(1) The dynamic system comprised of 2 state variables, global temperature and SLR, is a negative feedback system. This indicates that the rate of increase of temperature and SLR will decrease as their state values increase.

(2) The radiative forcing introduced on the system from CO_2 concentrations (ppmv) acts on the system as a power function with an exponent 1.31. This radiative forcing function accelerates the rise of global temperature at a rate of 0.10584°C $(W\ m^{-2})^{-1}$ yr^{-1}, which in turn increases the sea level in the dynamic system model. Therefore, reducing CO_2 emission is an effective way to control global warming and guarantee the sustainable development of coastal regions of the world.

Using the dynamic system model it is possible to estimate the direct impact of external forcing on the state variables. Using this concept, the emission controls necessary to either maintain or reduce future temperatures and sea levels may be calculated. This is a very important management issue which can be addressed through the use of the current model.

(3) The dynamic control system model provides a straightforward but effective approach to project the global temperature and SLR in the 21st century based on historical records.

LITERATURE CITED

Anderson MP, Woessner WW (1992) Applied groundwater modeling: simulation of flow and advective transport, 2nd edn. Academic Press, San Diego, CA

Aral MM, Guan J, Chang B (2012) A dynamic system model to predict global sea-level rise and temperature change. J Hydrol Eng 17:237–242

Church JA, White NJ (2006) A 20th century acceleration in global sea-level rise. Geophys Res Lett 33:L01602, doi: 10.1029/2005GL024826

Douglas BC (1997) Global sea rise: a redetermination. Surv Geophys 18:279–292

Draper NR, Smith H (1998) Applied regression analysis. Wiley, New York, NY

Etkins R, Epstein ES (1982) The rise of global mean sealevel as an indication of climate change. Science 215: 287–289

Gornitz V, Lebedeff S, Hansen J (1982) Global sea-level trend in the past century. Science 215:1611–1614

Grinsted A, Moore JC, Jevrejeva S (2010) Reconstructing sea level from paleo and projected temperatures 200 to 2100 ad. Clim Dyn 34:461–472

Hansen J, Sato M (2004) Greenhouse gas growth rates. Proc Natl Acad Sci USA 101:16109–16114

Hansen J, Sato M, Ruedy R, Lacis A, Oinas V (2000) Global warming in the twenty-first century: an alternative scenario. Proc Natl Acad Sci USA 97:9875–9880

Hansen J, Sato M, Ruedy R, Kharecha P and others (2007) Dangerous human-made interference with climate: a GISS modelE study. Atmos Chem Phys 7:2287–2312

Holgate S, Jevrejeva S, Woodworth P, Brewer S (2007) Comment on 'A semi-emprical approach to projecting future sea-level rise'. Science 317:1866

IPCC (2001) Climate change 2001: the scientific basis. Contribution of Working Group I to the Third Assessment Report of the Intergovernmental Panel on Climate Change. Cambridge University Press, Cambridge

IPCC (2007) Climate change 2007: the physical science basis. Contribution of Working Group I to the Fourth Assessment Report of the Intergovernmental Panel on Climate Change. Cambridge University Press, Cambridge

Jevrejeva S, Grinsted A, Moore JC (2009) Anthropogenic forcing dominates sea level rise since 1850. Geophys Res Lett 36:L20706, doi:10.1029/2009GL040216

Jevrejeva S, Moore JC, Grinsted A (2010) How will sea level response to changes in natural and anthropogenic forcings by 2100? Geophys Res Lett 37:L07703, doi:10.1029/2010GL042947

McLachlan GJ, Do KA, Ambroise C (2004) Analyzing microarray gene expression data. John Wiley & Sons, Hoboken, NJ

Meehl GA, Stocker TF, Friedlingstein WD, Collins P and others (2007) Projections of global average sea level change for the 21st century. In: Solomon S, Qin D, Manning M, Chen Z and others (eds) Climate change 2007: the physical science basis. Contribution of Working Group I to the fourth assessment report of the Intergovernmental Panel on Climate Change. Cambridge University Press, Cambridge, p 820–822

Pfeffer WT, Harper JT, O'Neel S (2008) Kinematic constraints on glacier contributions to 21st-century sea-level rise. Science 321:1340–1343

Rahmstorf S (2007) A semi-empirical approach to projecting future sea-level rise. Science 315:368–370

Rahmstorf S (2010) A new view on sea level rise. Nat Rep Clim Change 4:44−45

Schmith T, Johansen S, Thejil P (2007) Comment on 'A semi-empirical approach to projecting future sea-level rise'. Science 317:1866

Schmith T, Johansen S, Thejll P (2012) Statistical analysis of global surface temperature and sea level using cointegration methods. J Clim 25:7822−7833

Vermeer M, Rahmstorf S (2009) Global sea level linked to global temperature. Proc Natl Acad Sci USA 106: 21527−21532

von Storch H, Zorita E, González-Rouco JF (2008) Relationship between global mean sea-level and global mean temperature in a climate simulation of the past millennium. Ocean Dyn 58:227−236

Wadsworth HM (1998) Handbook of statistical methods for engineers and scientists, 2nd edn. McGraw-Hill, New York, NY

Editorial responsibility: Filippo Giorgi, Trieste, Italy

Submitted: January 23, 2013; Accepted: August 23, 2013
Proofs received from author(s): November 5, 2013